



ChemComm

---

**An Isolable Stannaimine and its Cycloaddition/Metathesis  
Reactions with Carbon Dioxide**

Journal:	<i>ChemComm</i>
Manuscript ID	CC-COM-08-2024-004006.R1
Article Type:	Communication

SCHOLARONE™  
Manuscripts

# An Isolable Stannamine and its Cycloaddition/Metathesis Reactions with Carbon Dioxide

Received 00th January 20xx,  
Accepted 00th January 20xx

Matthew J. Evans, Joseph M. Parr, Dat T. Nguyen, Cameron Jones\*

DOI: 10.1039/x0xx00000x

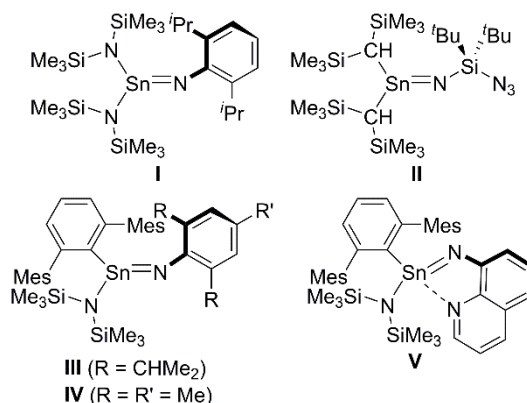
An *N*-heterocyclic stannylene,  $:\text{Sn}(\text{NON}^{\text{Ad}})$  ( $\text{NON}^{\text{Ad}} = [\text{O}(\text{SiMe}_2\text{NAd})_2]^{2-}$ , Ad = 1-adamantyl), reacts rapidly with 2,4,6-tricyclohexylphenyl azide (TCHP) $\text{N}_3$ , affording a stannamine,  $(\text{NON}^{\text{Ad}})\text{Sn}=\text{N}(\text{TCHP})$ . Solutions of  $(\text{NON}^{\text{Ad}})\text{Sn}=\text{N}(\text{TCHP})$  react immediately with carbon dioxide ( $\text{CO}_2$ ) to give a [2+2]-cycloaddition product, which, upon heating, subsequently engages in a metathesis process to give  $[\text{Sn}(\text{NON}^{\text{Ad}})(\mu\text{-O})]_2$  and the bulky isocyanate, (TCHP)NCO.

Atmospheric levels of  $\text{CO}_2$  continue to rise despite global efforts to limit emissions of this greenhouse gas.<sup>1</sup> Establishing methods to promote the stoichiometric and catalytic transformation of  $\text{CO}_2$  into less harmful value-added products is seen as an important step towards the mitigation of climate change.<sup>2</sup> Within this context, the selective activation of  $\text{CO}_2$  using main-group metal complexes has become an important objective of synthetic inorganic chemists.<sup>3</sup> While the trapping of  $\text{CO}_2$  within the coordination spheres of a host of main-group element complexes has been achieved, the utilisation of  $\text{CO}_2$  as a  $\text{C}_1$ -synthon to access useful chemical products has been comparatively less successful.<sup>4</sup> Main-group metal hydrides, particularly those of the *s*-block, have shown their capacity to effect the catalytic reduction of  $\text{CO}_2$ , yielding saturated products through hydrosilylation and hydroboration pathways.<sup>5</sup> There have also been considerable developments in the design of *s*-block and *p*-block catalysts for use in an array of other  $\text{CO}_2$  transformations.<sup>6</sup> Of some relevance to the current study, low oxidation state and Frustrated Lewis Pair (FLP) main-group systems have had some success in this arena.<sup>5a, 7</sup> With that said, the transformation of  $\text{CO}_2$  into useful organic products by main-group metal-element multiply bonded species has rarely been

documented.<sup>8</sup>

Stannamines, which incorporate a formal  $\text{Sn}=\text{N}$  bond, are typically synthesised through the reaction of a stannylene with an organic azide. Despite the structural authentication of the first stannamines (**I** and **II**) over three decades ago (Fig. 1),<sup>9</sup> their synthesis and isolation has proved problematic, largely due to their thermal instability and high reactivity.<sup>10</sup> A recent resurgence in stannamine chemistry has been spearheaded by Aldridge, Fischer and co-workers, who have demonstrated that a series of stannamines **III–V** can be kinetically stabilised by inclusion of sterically bulky *Sn*- and *N*-substituents, and these can be subsequently manipulated under ambient conditions.<sup>11</sup> As with related germanimines, stannamines **I** and **IV** show diverse reactivity towards small-molecule substrates (e.g. heteroallenes, ketones, alkynes).<sup>11–12</sup>

In this contribution, we report the syntheses and solid-state structural elucidations of both a monomeric *N*-heterocyclic stannylene and its dimeric distannene counterpart, which exist in equilibrium in solution. The reaction of this equilibrium mixture with a bulky azide affords a stannamine, which can be isolated and handled at room temperature, and can undergo a



metathesis reaction with  $\text{CO}_2$ , via an isolable [2+2] cycloadduct,

Fig. 1: Previously reported stannamines (I–V).

School of Chemistry, Monash University, Melbourne, PO Box 23, Victoria, 3800, Australia

Electronic supplementary information (ESI) available: Experimental procedures and characterisation data for all new compounds. Full details of computational studies. Crystal data, details of data collections and refinements. For ESI and crystallographic data in CIF or other electronic format see

DOI: 10.1039/x0xx00000x

thereby yielding a dimeric stannaoxane and a new isocyanate.

Stannylene :Sn(NON<sup>Ad</sup>) (**1**, NON<sup>Ad</sup> = [O(SiMe<sub>2</sub>NAd)<sub>2</sub>]<sup>2-</sup>, Ad = 1-adamantyl, Scheme 1) was obtained in moderate yield (54 %) through a two-step, one-pot reaction involving the lithiation of (NON<sup>Ad</sup>)H<sub>2</sub> with *n*-butyllithium followed by the addition of SnCl<sub>2</sub> in diethyl ether.<sup>13</sup> Interestingly, compound **1** crystallises as the stannylene from hexane solutions at elevated temperatures (> 342 K), while it is obtained in the solid-state as distannene [**1**]<sub>2</sub> from solutions at <243 K. Recrystallisation of **1** from hexane at room temperature affords co-crystallised **1** and [**1**]<sub>2</sub> (Figures S73–S75). For the stannylene (**1**), the Sn centre is chelated by the NON<sup>Ad</sup> ligand and there are no close Sn···Sn contacts (< 6 Å). The Sn–Sn bond (3.1448(5) Å) in [**1**]<sub>2</sub> is slightly longer than in the previously reported distannene [Sn(NON<sup>tBu</sup>)<sub>2</sub>] (3.1080(4) Å; NON<sup>tBu</sup> = [O(SiMe<sub>2</sub>NtBu)<sub>2</sub>]<sup>2-</sup>).<sup>13a</sup>

Distannenes and stannylens have been widely documented to exist in equilibrium in solution.<sup>14</sup> This appears to be the case for **1** and [**1**]<sub>2</sub>, though only marginal broadening of the ligand signals was observed in the <sup>1</sup>H NMR spectra of the equilibrium mixture across the temperature range 233 K – 353 K. This is mirrored in the <sup>119</sup>Sn{<sup>1</sup>H} NMR spectrum which exhibits a sharp singlet at δ<sub>Sn</sub> 806.6 ppm (233 K) and a broad singlet at δ<sub>Sn</sub> 842.7 (353 K). Lack of resolution into signals for both stannylene and distannene is consistent with related systems reported in the literature.<sup>15</sup>

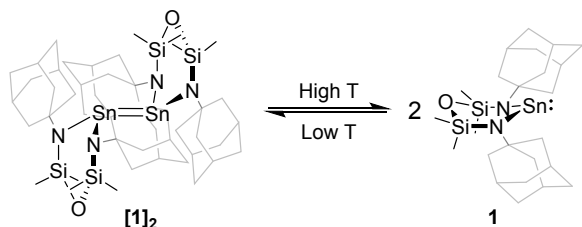
In line with the crystallographic and NMR spectroscopic studies on **1**, DFT studies at the MO6-2X level of theory show a negligible energy difference between the monomer **1** and dimer [**1**]<sub>2</sub> (ΔG<sup>o</sup><sub>298K</sub> = -0.2 kcalmol<sup>-1</sup>), with the distannene enthalpically favoured (ΔH<sup>o</sup><sub>298K</sub> = -15.3 kcalmol<sup>-1</sup>). The HOMO of **1** is best described as a carbene like Sn orbital of *p*-character, in plane with the Si–Sn–Si unit. The LUMO largely comprises a *p*-type orbital at Sn, which is orthogonal to the SnN<sub>2</sub> fragment. The

HOMO-LUMO gap was calculated as 5.84 eV (see ESI for computational details and molecular orbitals).

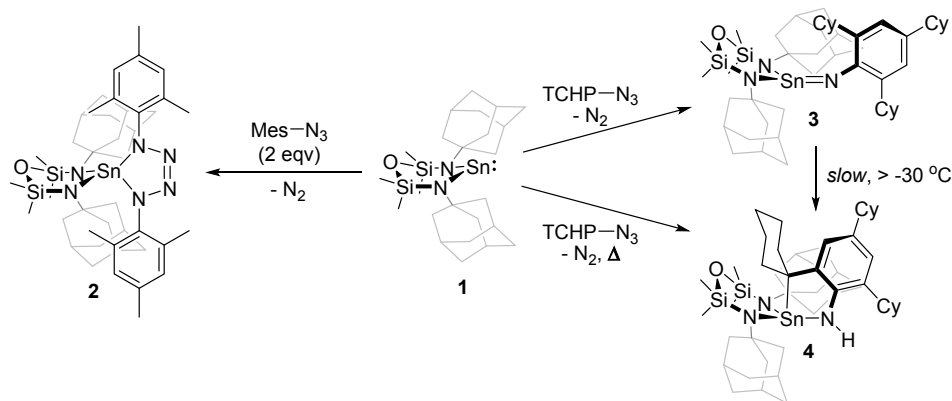
Similar to the situation in germanimine [(NON<sup>tBu</sup>)Ge=N(Mes)],<sup>16</sup> we envisaged that the NON<sup>Ad</sup> framework would allow stabilisation of a related stannimine.<sup>13b</sup> Initial attempts to isolate a stannimine from the reaction of mesityl azide with **1** (*cf.* **IV**) were unsuccessful due to onward reactivity giving stannatetrazole **2** (Scheme 2). The solid-state structure of **2** (Figure S76) is reminiscent of solution-state NMR spectroscopic data obtained on isolated crystals of the compound. With this result in mind, we set out to design a bulkier azide that would be suitable for the kinetic stabilisation of an Sn=N bond. We have previously shown that the bulky 2,4,6-tricyclohexylphenyl moiety is a particularly useful ligand substituent for the isolation of highly reactive main-group species.<sup>5a, 17</sup> Accordingly, here we prepared 2,4,6-tricyclohexylphenyl azide utilising a 2-step procedure from 2,4,6-tricyclohexylphenyl bromide (see ESI for further details).

The addition of 2,4,6-tricyclohexylphenyl azide to a solution of **1** resulted in vigorous gas evolution and the formation of a deep red solution. Storage of this solution at -30 °C for 18 hours provided dark red crystals of **3** in moderate isolated yield (45%). The solid-state structure of **3** (Fig. 2) reveals a trigonal planar geometry at the Sn centre, with a short Sn=N bond (1.9337(15) Å) within the range of previously reported stannimine systems (1.905(5) – 2.022(4) Å).<sup>9a, 9b, 11</sup> The electronic structure of **3** was investigated by DFT, and was found to be comparable to that calculated for **III–V** by Fischer, Aldridge and co-workers.<sup>11</sup> The HOMO-1 and LUMO of **3** consist of the Sn=N π-bonding and π-antibonding orbitals, respectively. A Natural Bonding Orbital (NBO) analysis points to a highly polarised Sn–N bond, with calculated charges for Sn and N of +2.21 and -1.14, respectively. The Sn–N Wiberg bond index was calculated as 1.05. ETS-NOCV calculations, fragmenting **3** at the Sn=N bond, show a total orbital interaction energy (ΔE<sub>ORB</sub>) of -243.7 kcalmol<sup>-1</sup>, with the principal contribution corresponding to donation from the Sn to N atom (Δp<sup>1</sup> = -183.2 kcalmol<sup>-1</sup>, 75% of ΔE<sub>ORB</sub>).

Although **3** is stable in the solid-state for days at room temperature, allowing a solution of the compound to stand at 298 K for <1 day gave a pale red-orange solution, from which colourless crystals of **4** could be isolated. The structure of **4** indicates that **3** has undergone C–H activation at the α-carbon of an *ortho*-cyclohexyl group, to form a 5-membered



**Scheme 1:** Solution-state equilibrium between stannylene **1** and distannene [**1**]<sub>2</sub>.



**Scheme 2:** Synthesis of stannatetrazole **2** and stannimine **3**. Rearrangement of **3** to form C–H activated product **4**. Note: **1** drawn as the stannylene for simplicity.

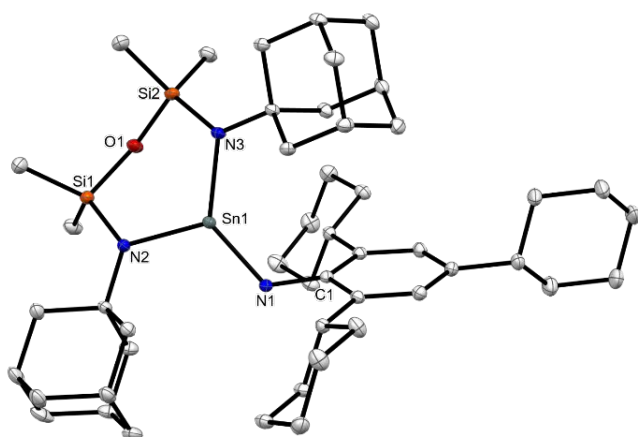


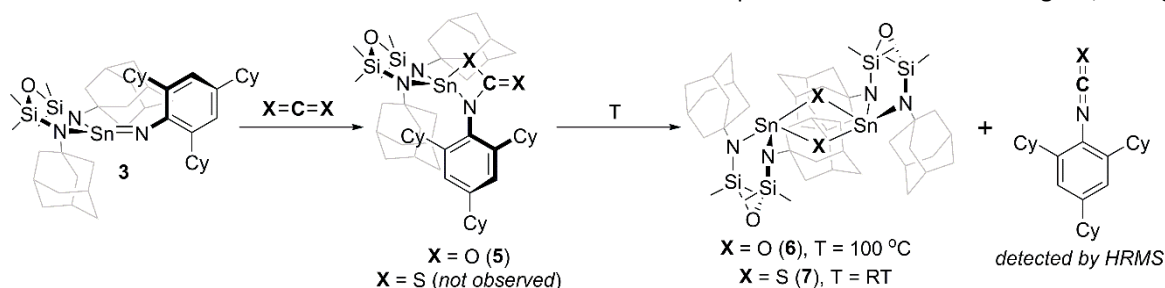
**Fig. 2:** Molecular structure of (NON<sup>Ad</sup>)Sn=N(TCHP) **3**. Thermal ellipsoids shown at 20% probability; hydrogen atoms omitted. Selected bond lengths (Å) and angles (°): Sn(1)–N(1) 1.9337(15), Sn(1)–N(2) 2.0267(15), Sn(1)–N(3) 2.0462(15), N(1)–C(1) 1.398(2), N(2)–Sn(1)–N(3) 111.72(6), Sn(1)–N(1)–C(1) 123.06(12).

metallacycle (Figure S78). This is further supported by the <sup>1</sup>H NMR spectrum of the compound, which is consistent with a low-symmetry species, and which exhibits an NH signal at  $\delta_H$  3.97 ppm (s, 1H). Although the C–H activation of cyclohexyl groups is rare,<sup>18</sup> intramolecular C–H activation events are not uncommon for stannamines, and appear to be the primary decomposition mode for previously reported **I** and **III–V**.<sup>9a, 11</sup> Intramolecular C–H activation of **3** was calculated to be highly exergonic, consistent with an irreversible process, as observed experimentally ( $\Delta G^\circ_{298K} = -38.8$  kcalmol<sup>-1</sup>).

As stannamines and germanimines have been reported to engage in [2+2]-cycloaddition reactions with CO<sub>2</sub><sup>11, 12b</sup> and

metathesis-type reactions with other heteroallenes to generate organic products,<sup>11–12</sup> we proceeded to investigate the reactivity of **3** towards CO<sub>2</sub>. Exposure of solutions of **3** to an atmosphere of CO<sub>2</sub> resulted in an immediate colour change from dark red to colourless. Crystals of **5** were obtained from the reaction mixture in moderate yield (51%) after work-up (Scheme 3). In the solid-state, the Sn centre of **5** adopts a distorted tetrahedral geometry with coordination to the NON<sup>Ad</sup> and [OC(O)N(TCHP)]<sup>2-</sup> ligands, the latter of which is consistent with a [2+2]-cycloaddition of a C=O bond of CO<sub>2</sub> across the Sn=N bond in **3** (Fig. 3a). The <sup>13</sup>C{<sup>1</sup>H} NMR spectrum of **5** displays a diagnostic signal for the installed CO<sub>2</sub> fragment at  $\delta_c$  160.8 ppm, which is further validated by a strong C=O stretch at 1692 cm<sup>-1</sup> in the infrared spectrum of the compound.

Heating a solution of **5** in C<sub>6</sub>D<sub>6</sub> at 100 °C for 72 hours resulted in the deposition of colourless crystals and the disappearance of signals due to the NON<sup>Ad</sup> ligand in the <sup>1</sup>H NMR spectrum of the mother liquor. Analysis of the colourless crystals by an X-ray diffraction experiment revealed them to be the dimeric stannaoxane **6** (Scheme 3). The coordination environment of the Sn centre of **6** is fulfilled by bonding to the NON<sup>Ad</sup> and  $\mu$ -O<sup>2-</sup> ligands resulting in a distorted tetrahedral geometry (Fig. 3b). Once **6** was isolated by filtration, analysis of the remaining solution by HRMS indicated the presence of 2,4,6-tricyclohexylphenyl isocyanate (TCHP)NCO. Attempts to crystallise this product by slow evaporation of a C<sub>6</sub>D<sub>6</sub> solution instead gave a small number of colourless crystals of 1-(1-adamantyl)-3-(2,4,6-tricyclohexylphenyl)urea (TCHP-NH-CO-NH-Ad, Figure S80). We suspect that a portion of the generated (TCHP)NCO reacts with an equivalent of Ad-NH<sub>2</sub>, which arises from decomposition of the NON<sup>Ad</sup> ligand, to give the



**Scheme 3:** Utilisation of **3** in cycloaddition, and subsequent metathesis reactions of CO<sub>2</sub> and CS<sub>2</sub>, yielding isocyanate and isothiocyanate products.

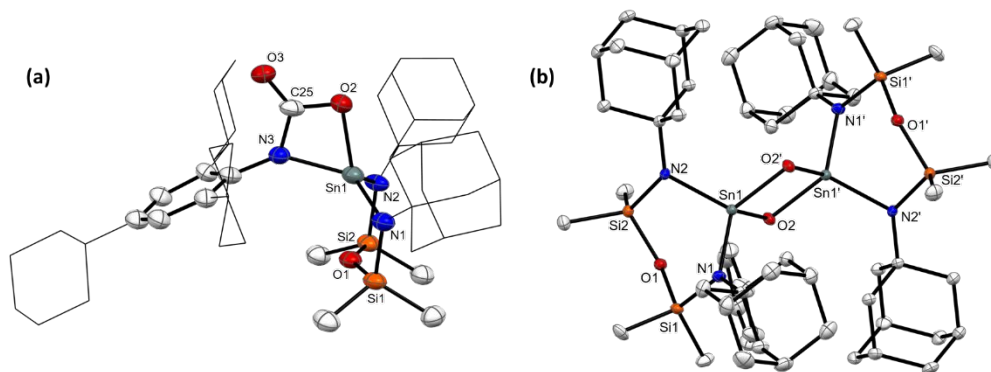


**Fig. 3:** Molecular structures of **5** (a) and **6** (b). Thermal ellipsoids shown at 20% probability; hydrogen atoms omitted; cyclohexyl and adamantyl groups shown in wireframe for **5** for clarity. ' = 1-x, 1-y, -z. Selected bond lengths (Å) for **5**: Sn(1)–O(2) 2.044(6), Sn(1)–N(3) 2.070(7), C(25)–N(3) 1.378(10), C(25)–O(2) 1.330(12), C(25)–O(3) 1.231(11); for **6**: Sn(1)–O(2) 1.9826(19), Sn(1)–O(2') 2.0134(19).

unsymmetrical urea species. This is not unexpected as isocyanates are commonly utilised in the synthesis of symmetrical and unsymmetrical ureas.<sup>19</sup>

The scope of this reaction was explored further in the reaction of carbon disulphide (CS<sub>2</sub>) with **3**, which resulted in the formation of stannathione **7**. This formed directly, without a cycloaddition intermediate (cf. **5**) being isolable. DFT studies showed that the transformation of **3** to **7** is highly exergonic (with respect to **3** to **6**), which is perhaps why the intermediate [2+2]-cycloaddition product was not observed (see ESI for details). Compound **7** is isostructural to **6**, and as such, its structure will not be discussed here (Figure S79). An assay of the crude reaction mixture that gave **7** by HRMS showed the presence of 2,4,6-tricyclohexylphenyl isothiocyanate, (TCHP)NCS, consistent with the proposed metathesis of CS<sub>2</sub>.

In summary, we have synthesised a stannylene and distannene, :Sn(NON<sup>Ad</sup>) **1** and [Sn(NON<sup>Ad</sup>)]<sub>2</sub> [**1**]<sub>2</sub>, which react with 2,4,6-tricyclohexylphenyl azide to afford a highly reactive stannamine, (NON<sup>Ad</sup>)Sn=N(TCHP) **3**. The activation of CO<sub>2</sub> by **3** proceeds via an initial [2+2]-cycloaddition reaction, followed by metathesis under thermal conditions, generating a dimeric stannaoxane and 2,4,6-tricyclohexylphenyl isocyanate. We suspect that bulky 2,4,6-tricyclohexylphenyl azide may find application in the stabilization of other challenging and previously inaccessible main-group imido compounds.

C. J. thanks the Australian Research Council for funding. In addition, this material is based upon work supported by the Air Force Office of Scientific Research under award number FA2386-21-1-4048. We wish to acknowledge Dr. Alasdair McKay (NMR), Dr. Boujemaa Moubaraki (HRMS), and Dr. Craig Forsyth (SC-XRD) for their services to the Monash Analytical Platform (MAP). M. J. E. thanks Dr. Dominic Kennedy for moral support. We also wish to acknowledge the Australian Synchrotron for access to the MX1 and MX2 beamlines, and their beamline scientists.

## Data availability

The data supporting this article have been included as part of the ESI.

## Conflicts of interest

There are no conflicts to declare.

## Notes and references

- Z. Liu, Z. Deng, S. Davis and P. Ciais, *Nat. Rev. Earth Environ.*, 2023, **4**, 205-206.
- a) M. Mikkelsen, M. Jørgensen and F. C. Krebs, *Energy Environ. Sci.*, 2010, **3**, 43-81; b) T. Sakakura, J.-C. Choi and H. Yasuda, *Chem. Rev.*, 2007, **107**, 2365-2387.
- a) M. Pérez-Jiménez, H. Corona, F. de la Cruz-Martínez and J. Campos, *Chem. Eur. J.*, 2023, **29**, e202301428; b) S. Sinha and J. J. Jiang, *Chem. Commun.*, 2023, **59**, 11767-11779; c) P. P. Power, *Nature*, 2010, **463**, 171-177.
- C. Weetman and S. Inoue, *ChemCatChem*, 2018, **10**, 4213-4228.
- a) M. J. Evans and C. Jones, *Chem. Soc. Rev.*, 2024, **53**, 5054-5082; b) M. M. D. Roy, A. A. Omaña, A. S. S. Wilson, M. S. Hill, S. Aldridge and E. Rivard, *Chem. Rev.*, 2021, **121**, 12784-12965.
- a) Q. Liu, L. Wu, R. Jackstell and M. Beller, *Nat. Commun.*, 2015, **6**, 5933; b) C. Maeda, Y. Miyazaki and T. Ema, *Catal. Sci. Technol.*, 2014, **4**, 1482-1497.
- a) M. Asay, C. Jones and M. Driess, *Chem. Rev.*, 2011, **111**, 354-396; b) R. Akhtar, K. Gaurav and S. Khan, *Chem. Soc. Rev.*, 2024, **53**, 6150-6243; c) M. P. Coles and M. J. Evans, *Chem. Commun.*, 2023, **59**, 503-519; d) M. He, C. Hu, R. Wei, X.-F. Wang and L. L. Liu, *Chem. Soc. Rev.*, 2024, **53**, 3896-3951; e) F.-G. Fontaine, M.-A. Courtemanche, M.-A. Légaré and É. Rochette, *Coord. Chem. Rev.*, 2017, **334**, 124-135; f) D. W. Stephan and G. Erker, *Chem. Sci.*, 2014, **5**, 2625-2641; g) D. W. Stephan, *Acc. Chem. Res.*, 2015, **48**, 306-316.
- C. Weetman, *Chem. Eur. J.*, 2021, **27**, 1941-1954.
- a) G. Ossig, A. Meller, S. Freitag and R. Herbst-Irmer, *J. Chem. Soc., Chem. Commun.*, 1993, 497-499; b) T. Ohtaki, Y. Kabe and W. Ando, *Hetero. Chem.*, 1994, **5**, 313-320; c) J. Barrau, G. Rima and T. El Amraoui, *J. Organomet. Chem.*, 1998, **570**, 163-174.
- a) A. Schulz, M. Thomas and A. Villinger, *Dalton Trans.*, 2019, **48**, 125-132; b) U. Fookien, W. Saak and M. Weidenbruch, *J. Organomet. Chem.*, 1999, **579**, 280-284; c) H. Grützmacher and H. Pritzkow, *Angew. Chem. Int. Ed. Engl.*, 1991, **30**, 1017-1018; d) P. Švec, Z. Padělková, M. Alonso, F. De Proft and A. Růžicka, *Can. J. Chem.*, 2014, **92**, 434-440; e) R. Guthardt, L. Oetzel, T. Lang, C. Bruhn and U. Siemeling, *Chem. Eur. J.*, 2022, **28**, e202200996.
- M. Fischer, M. M. D. Roy, L. L. Wales, M. A. Ellwanger, C. McManus, A. F. Roper, A. Heilmann and S. Aldridge, *Angew. Chem. Int. Ed.*, 2022, **61**, e202211616.
- a) G. Ossig, A. Meller, S. Freitag, R. Herbst-Irmer and G. M. Sheldrick, *Chem. Ber.*, 1993, **126**, 2247-2253; b) M. J. Evans, F. M. Burke, P. M. Chapple and J. R. Fulton, *Inorg. Chem.*, 2021, **60**, 8293-8303.
- a) R. J. Schwamm, C. A. von Randow, A. Mouchfiq, M. J. Evans, M. P. Coles and J. Robin Fulton, *Eur. J. Inorg. Chem.*, 2021, **2021**, 3466-3473; b) D. T. Nguyen, M. J. Evans and C. Jones, *J. Organomet. Chem.*, 2024, **1012**, 123143.
- W. Zou, M. Bursch, K. L. Mears, C. R. Stennett, P. Yu, J. C. Fettinger, S. Grimme and P. P. Power, *Angew. Chem. Int. Ed.*, 2023, **62**, e202301919.
- a) J. Henoch, A. Auch, F. Diab, K. Eichele, H. Schubert, P. Sirsch, T. Block, R. Pöttgen and L. Wesemann, *Inorg. Chem.*, 2018, **57**, 4135-4145; b) K. L. Mears and P. P. Power, *Chem. Eur. J.*, 2023, **29**, e202301247; c) C. R. Stennett, M. Bursch, J. C. Fettinger, S. Grimme and P. P. Power, *J. Am. Chem. Soc.*, 2021, **143**, 21478-21483.
- M. J. Evans, M. D. Anker, A. Mouchfiq, M. Lein and J. R. Fulton, *Chem. Eur. J.*, 2020, **26**, 2606-2609.
- a) R. Mondal, M. J. Evans, T. Rajeshkumar, L. Maron and C. Jones, *Angew. Chem. Int. Ed.*, 2023, **62**, e202308347; b) R. Mondal, K. Yuvaraj, T. Rajeshkumar, L. Maron and C. Jones, *Chem. Commun.*, 2022, **58**, 12665-12668.
- A. E. W. Ledger, M. F. Mahon, M. K. Whittlesey and J. M. J. Williams, *Dalton Trans.*, 2009, 6941-6947.
- C. Six and F. Richter, in *Ullmann's Encyclopedia of Industrial Chemistry*, 2003.

**Data Availability Statement**

The data supporting this article have been included as part of the ESI.